Received: 18 October 2019 | Revised: 17 March 2020 | Accepted: 23 March 2020

DOI: 10.1096/fj.201902630R

RESEARCH ARTICLE

THE FASEB JOURNAL

Organism dual RNA-seq reveals the importance of BarA/UvrY in *Vibrio parahaemolyticus* virulence

Wenwen Zhang[1] | **Ruiqiang Xie**[1] | **Xiaohua Douglas Zhang**[1] | **Leo Tsz On Lee**[1] | **Hongjie Zhang**[1] | **Menghua Yang**[2] | **Bo Peng**[3,4] | **Jun Zheng**[1,5]

[1]Faculty of Health Sciences, University of Macau, Macau SAR, China

[2]Key Laboratory of Applied Technology on Green-Eco-Healthy Animal Husbandry of Zhejiang Province, College of Animal Science and Technology, Zhejiang A&F University, Hangzhou, China

[3]Laboratory for Marine Biology and Biotechnology, Qingdao National Laboratory for Marine Science and Technology, Qingdao, China

[4]School of Life Sciences, Sun Yat-sen University, Guangzhou, China

[5]Institute of Translational Medicine, University of Macau, Macau SAR, China

Correspondence
Jun Zheng, Faculty of Health Sciences, University of Macau, Macau SAR, China.
Email: Junzheng@um.edu.mo

Abstract

Elucidation of host-pathogen interaction is essential for developing effective strategies to combat bacterial infection. Dual RNA-Seq using cultured cells or tissues/organs as the host of pathogen has emerged as a novel strategy to understand the responses concurrently from both pathogen and host at cellular level. However, bacterial infection mostly causes systematic responses from the host at organism level where the interplay is urgently to be understood but inevitably being neglected by the current practice. Here, we developed an approach that simultaneously monitor the genome-wide infection-linked transcriptional alterations in both pathogenic *Vibrio parahaemolyticus* and the infection host nematode *Caenorhabditis elegans*. Besides the dynamic alterations in transcriptomes of both *C. elegans* and *V. parahaemolyticus* during infection, we identify a two-component system, BarA/UvrY, that is important for virulence in host. BarA/UvrY not only controls the virulence factors in *V. parahaemolyticus* including Type III and Type VI secretion systems, but also attenuates innate immune responses in *C. elegans*, including repression on the MAP kinase-mediated cascades. Thus, our study exemplifies the use of dual RNA-Seq at organism level to uncover previously unrecognized interplay between host and pathogen.

KEYWORDS

C. elegans, organism dual RNA-Seq, BarA, UvrY, *V. parahaemolyticus*, virulence factor

1 | INTRODUCTION

Bacterial pathogens encounter changes in the environmental condition during their infections. Both eukaryotic host cells and bacteria would initiate a dynamic cascade of events that culminates in the altered gene expression patterns for survival. A comprehensive understanding on the transcriptomes of both host and pathogen can provide new insights into this process and enable the identification of new virulence factors in the pathogen or new regulation cascades in the host that are responding to the attack by the specific pathogens. RNA sequencing (RNA-Seq) is a powerful technology developed for global gene expression analysis during pathogen infection. However, traditional RNA-Seq has outstanding limitation on the studies of host-pathogen interaction: it is restricted to transcriptome of either the pathogen or the host at a time and could not provide a full picture of dynamic

Abbreviations: CsrB, carbon storage regulator B; qRT-PCR, quantitative real-time PCR; RNA-Seq, RNA sequencing; T3SS, type III secretion system; T6SS, type VI secretion system.

interacting responses between bacteria and host during the infection.[1] This weak point has been overcome by the conceptual introduction of "dual RNA-Seq".[2-5] Instead of physically separation of the pathogen from infected host cells, the transcriptomes from both host and pathogen will be sequenced together and only be distinguished subsequently by in silico analysis.[1,5] This technology has been widely used and become a powerful approach to reveal many novel mechanisms on the interaction between host and pathogens.[6-9]

While many novel insights into the cross-talk between pathogen and host have been disclosed by this technology, the use of cultured cells or tissues/organs have inevitably neglected the host responses at the organism level.[2-4] Conducting dual RNA-Seq with whole-animal would provide additional information on bacteria-host interaction. However, the traditional animal model for bacterial infection, such as mouse or Zebrafish, are not suitable for dual RNA-Seq at organism level due to their relatively large size. The nematode *Caenorhabditis elegans* is a simple model for studying bacteria-host interaction. It is small in size, and the adult worm only have around a thousand cells. Importantly, *C. elegans* is similar in various aspects to mammalian hosts. *C. elegans* have been used as a model to investigate the bacterial pathogenesis in a remarkable large number of human microbial pathogens, including *vibrio* species, such as *V. cholerae* and *Vibrio vulnificus*.[10,11]

Vibrio parahaemolyticus is a Gram-negative halophilic bacterium that is commonly found in estuarine, marine, and coastal environments.[12] It is an emerging bacterial pathogen and a leading cause of human gastroenteritis associated with seafood consumption throughout the world.[12,13] However, the pathogenicity of *V. parahaemolyticus* has not been fully elucidated.[14] The major virulence factors that have been characterized so far include adhesins,[15] thermostable direct hemolysin (TDH), and TDH-related hemolysin (TRH)[16,17] as well as two type III secretion systems, namely T3SS1 and T3SS2,[18] and the polar and lateral flagella.[19-21] Each T3SS secretes a unique set of effectors that contribute to the virulence by acting on different host targets and serves different functions. T3SS1 causes cytotoxicity, whereas T3SS2 is mainly associated with enterotoxicity.[18] In addition, *V. parahaemolyticus* contains two type VI secretion systems (T6SS1 and T6SS2), among which T6SS2 has also been implicated in the bacterial pathogenesis.[22]

In this study, we established an organism dual RNA-Seq with *C. elegans* as an infection host for pathogenic *V. parahaemolyticus*. We have successfully applied this approach to investigate the global dynamic gene expression alterations of both *V. parahaemolyticus* and *C. elegans* during the infection process. Our results revealed insights into the infection stimuli that provoke the gene expression changes driving bacterial pathogenesis and the corresponding host responses at organism level. We discovered the important role of the two-component system BarA/UvrY in bacterial pathogenesis through controlling bacterial virulence factors. Importantly, the simultaneous monitoring on bacteria-host responses also enabled us to identify the repression of host innate immunity responses by *V. parahaemolyticus* through BarA/UvrY.

2 | MATERIALS AND METHODS

2.1 | Bacterial strains, plasmids, and growth conditions

The bacterial strains and plasmids used in this study are listed in Dataset S1. LB broth was used for all the experiments. Culture media were supplemented with ampicillin (Amp, 50 μg/mL) or chloramphenicol (Chl, 20 μg/mL) when necessary.

2.2 | Construction of bacterial strains and plasmids

In-frame deletion mutants were constructed by the *SacB*-based allelic exchanges as previously described with plasmid pDS132.[23,24] Briefly, for construction of Δ*uvrY*, primer sets of *uvrY*_L_F/*uvrY*_L_R and *uvrY*_R_F/*uvrY*_R_R were used to amplify the upstream and downstream fragments of *uvrY*. A 20-bp overlap in the sequences of each PCR products introduced by primers of *uvrY*_L_R and *uvrY*_R_F permitted a second amplification of about 1800-bp product containing about 900-bp fragment upstream of *uvrY* and about 900-bp fragment downstream of the *uvrY,* respectively, by the primers of *uvrY*_L_F and *uvrY*_R_R. The resultant fragment was ligated into *Xba*I-digested plasmid pDS132 using the In-Fusion HD Cloning kit (Clontech) following the user manual. The resultant plasmid was mobilized into *V. parahaemolyticus* cells by *Escherichia coli* DH5αλpir. Double cross-over mutants were selected on LB agar plates supplemented with 10% sucrose. The deletion mutants were verified by PCR. The construction of other deletion mutants and the chromosomal *uvrY:: 3 × FLAG* in *V. parahaemolyticus* followed a similar procedure. Complementation of mutants were achieved by the expression of the corresponding WT gene on plasmid pBAD24-cm, a pBAD24 derivative in which the ampicillin resistant gene was replace by chloramphenicol. Then, transforming corresponding pBAD24-cm to the mutant strain by a triparental mating with a helper strain of *E. coli* DH5α containing pRK2073. Oligonucleotides used for plasmid and mutant construction are listed in Dataset S1.

2.3 | *C. elegans* maintenance and nematode lethality assay

C. elegans WT strain Bristol N2 was maintained at 23°C on nematode growth medium (NGM) agar plates seeded with *E.*

coli OP50 following the standard method.[25] The nematode lethality assay was performed as described previously with minor modification.[26,27] Briefly, bacteria from overnight culture were directly inoculated into the liquid media at 1:100 into 6-well microtiter dish containing 2 mL of liquid media (80% M9 and 20% BHI). The L4 stage of *C. elegans* were washed with M9 minimal media (22 mM KH_2PO_4, 42 mM Na_2HPO_4, 86 mM NaCl, and 1 mM $MgSO_4$) and then approximately 15 to 30 worms were transferred into each well. Plates were incubated at 23°C and the live worms in the well were recorded every day. The worms were considered to be dead if they do not move or exhibit muscle tone during the shaking of 6-well plate by hands.

2.4 | Bacterial colonization and accumulation in nematodes

Nematodes infected with GFP-labeled bacteria were investigated by fluorescent microscopy as previously described.[28] Plasmid expressing GFP was mobilized into *V. parahaemolyticus* by triparental mating technique.[29] Briefly, *C. elegans* infected with bacteria expressing GFP were washed five times by M9 buffer. The washed worm was eventually resuspended in M9 buffer supplemented with 30 mM sodium azide (Sigma) as the anaesthetic. The colonization of bacteria in worm was then examined using a Carl Zeiss microscope.

Bacterial accumulation in worm was quantified followed previous description.[30] Worms infected for duration as indicated in the text were collected and washed three times with M9 buffer containing 1mM sodium azide and 100 μg/mL of gentamicin. Worms were then incubated with the same buffer for 1 hour to kill the bacteria on the worm surface and inhibit the expulsion of bacteria from the worm intestine. The infected worms were washed three times again with M9 buffer. Approximately 10 worms were transferred into a 2 mL of micro-centrifuge tube and M9 buffer was added up to a final volume of 1 mL. Approximately 400 mg of 1.0 mm silicon carbide particles (Thermo Fisher Scientific) were added to the tube, which was then vortexed at maximum speed for 1 minute to completely disrupt the worms to release bacteria. The resulting suspension was diluted and plated onto LB agar to determine bacterial colony forming units (CFU).

2.5 | Infection of *C. elegans* for organism dual RNA-Seq

The L4 stage of *C. elegans* were infected by bacteria according to the same procedure as described in nematode lethality assay. Briefly, *C. elegans* infected by bacteria for 12, 24, 36, 48 hours as indicated in the text were collected and washed three times with M9 buffer containing 1 mM sodium azide and 100 μg/mL of gentamicin for 1 hour to kill the bacteria on the worm surface and to inhibit the expulsion of bacteria from the worm intestine. Total RNA was then isolated from *C. elegans* containing bacteria using the mirVana kit (Ambion) following the user manual. The isolated total RNA was treated with DNase I (Fermentas) (0.25 U/1 μg of RNA) for 30 mins, followed by purification with ethanol. The Ribo-Zero Magnetic Gold Kit (Epidemiology) from Epicentre/Illumina was used to remove rRNA in the samples following the manufacturer's instructions. The success removal of rRNA was examined by Agilent RNA6000 Pico kit.

cDNA libraries for Illumina sequencing were constructed with NEBNext Ultra Directional RNA Library Prep Kit for Illumina (E7420) following the manufacture instruction. For organism dual RNA-Seq, ~100 ng rRNA-depleted RNA were used for cDNA library preparation. cDNA library quality was assessed with Agilent High Sensitivity DNA Chip and samples demonstrating a narrow distribution with a peak size approximately 200-800 bp were accepted.

2.6 | Reads mapping and data analysis

The reads' quality was assessed first by FastQC.[31] Then the raw data of reads from mixed RNA-Seq libraries were mapped to *V. parahaemolyticus* RIMD2210633 and *C. elegans* genome using TopHat2[32] with the default parameterization, respectively. The corresponding mapped reads were categorized as reads from *V. parahaemolyticus* and *C. elegans* for the subsequent analysis. Reads aligned to annotated genes were quantified with the htseq-count program using gene annotations from Ensembl 92. Determined uniquely mapped read counts were served as input to DESeq2 (version 1.14.1) for pairwise detection and quantification of differential gene expression with default parameterization.[33] The list of DESeq2 determined differentially expressed genes (DEGs) was filtered with a conservative absolute log2 with fold change cutoff of 1 for bacteria and 0.6 for *C. elegans*. Lists of differentially expressed genes were further annotated with the pathway information from the KEGG and WormBase database. The COG function of genes in *V. parahaemolyticus* were predicted by EggNOG database. R basic package was used to generate heat map and boxplot.

2.7 | Quantitative real-time PCR

Quantitative real-time PCR (qRT-PCR) was performed using the 7500 Real-Time PCR system (Applied Biosystems) to examine the gene expression level. The RNA extraction follows the same procedure in organism dual RNA-Seq. Random hexamers (Sigma) were used for reverse transcript. FastStart Universal SYBR Green Master mix (Takara) was

used to perform qRT-PCR. The fold change in target gene relative to the housekeeping gene (16S rRNA for bacteria or β-actin for *C. elegans*) was determined by the $2^{-\Delta\Delta Ct}$ method. At least two biological replicates were performed for each qRT-PCR analysis. The experiment repeated at least twice. Primers used for qRT-PCR are shown in Dataset S1.

2.8 | Mammalian cell culture and Infection

HeLa cells were grown in high-glucose Dulbecco's modified Eagle's Medium (DMEM) (Gibco) supplemented with 10% fetal bovine serum (FBS, Gibco) at 37°C with 5% CO_2. The infection of HeLa cells by *V. parahaemolyticus* was performed following previous description.[34] Briefly, HeLa cells were seeded into 6-well tissue culture plates containing coverslips at 1×10^5 cells per well at 24 hours before infection. HeLa cells were infected by bacteria at MOI of 10. At different time point post infection as indicated in the text, HeLa cells were washed with 1 × phosphate-buffered saline (PBS) and then fixed by 3.2% (v/v) paraformaldehyde for 15 minutes, followed by permeabilization with 0.1% (w/v) Triton X-100 for 15 minutes at room temperature. F-actin and DNA of HeLa cells was stained with Alexa Fluor 488–phalloidin (2 U/mL; Thermo Fisher Scientific) and Hoechst A33342 (1 mg/mL; Invitrogen), respectively. Coverslips were mounted on glass slides with ProLong Gold Antifade mounting medium (Thermo Fisher Scientific) and cells were imaged with a Zeiss microscope. Images were processed with ZEN 2 software (Zeiss).

To conduct cytotoxicity assay, HeLa cells seeded in 96-well plate were washed by unsupplemented DMEM (DMEM without FBS). Fresh mid-log bacteria cultured at 23°C ($OD_{600} \approx 0.5$) were washed with 1 × PBS briefly and re-suspended with two volumes of unsupplemented DMEM. HeLa cells were then infected by bacteria at an MOI of 10. Cytotoxicity was determined with CytoTox 96® Reagent (Promega) following manufacture's user manual.

2.9 | ChIP-Seq with UvrY-3 × FLAG

ChIP (chromatin immunoprecipitation) was performed following previous description[35,36] with minor modifications. Briefly, 6 mL of bacterial cells were cross-linked with formaldehyde (1%) for 25 minutes at room temperature. Glycine (0.2M) was then added to the mixture, followed by 15 minutes incubation at room temperature to stop the reaction. Bacteria were washed with pre-cold 1 × PBS and lysed by sonication in 500 μL of lysis buffer (50 mM HEPES-KOH, 150 mM NaCl, 1 mM EDTA, 10 mL of Triton-100, 0.1% sodium deoxycholate, and 0.1% SDS). The bacterial debris was removed by centrifugation at 13 000 rpm for 30 minutes at 4°C. The supernatant was then used for immunoprecipitation using Protein A Dynabeads (GE Healthcare, 17-0963-03) following the manufacture instruction. QIAquick PCR Purification Kit was used to collect the DNA sample, using TE buffer to resolve the DNA. The collected DNA was kept at 4°C for ChIP-Seq cDNA library preparation. cDNA libraries for Illumina sequencing were constructed with NEBnext Ultra II DNA Library Pre Kit for Illumina (E7645) following the user manual.

To conduct ChIP-qPCR, 10% of each sample was removed after the pre-cleaning step and the extracted DNA served as the input. About 1 μL of ChIP samples and diluted input samples were served as templates for qPCR performed with primers annealing upstream of the potential *uvrY*-regulated genes. The IP efficiency was calculated as follows: IP efficiency = 100/2^ΔCq [normalized ChIP] where ΔCq [normalized ChIP] = Cq [ChIP] − (Cq[input] − log2[input dilution factor]). The fold enrichment of the target = IP efficiency of the target /IP efficiency of the background. Oligonucleotides used for CHIP-qPCR are listed in Dataset S1.

2.10 | Protein assay

Secreted proteins were extracted from fresh bacterial culture ($OD_{600} = 0.9$) grown in LB broth.[37] Briefly, bacteria were incubated at 23°C with agitation of 220 rpm till OD_{600} reached 0.9, and 0.2% arabinose was added when necessary to induce the expression of tested protein for 2 hours. Bacteria were pelleted by centrifugation and the supernatant was used to isolate the secreted proteins by trichloroacetic acid–acetone (TCA) precipitation. Pelleted bacteria were resuspended in lysis buffer (100 mM Tris-HCl pH 6.8, 3.2% SDS, 3.2 mM EDTA, 16% glycerol, 0.2 mg/mL of bromophenol blue, and 2.5% β-mercaptoethanol). Proteins extracted were separated by 10% SDS-PAGE, followed by Western blot analysis.

2.11 | Zebrafish intraperitoneal injection assay

Adult Zebrafish was acclimated at room temperature for 1 week before infection treatment. Bacteria were intraperitoneally injected into Zebrafish following previous protocol.[38] Briefly, Zebrafish was anesthetized with 1% Ethyl 3-aminobenzoate methane sulfonate (Sigma) first, and 20 μL of bacteria with approximately 1.0×10^6 CFU/mL were intraperitoneally injected into the midline of the abdomen immediately posterior to the pectoral fins. Infected Zebrafish were transferred to a freshwater tank. Fish was observed for 4 days and their mortalities were recorded.

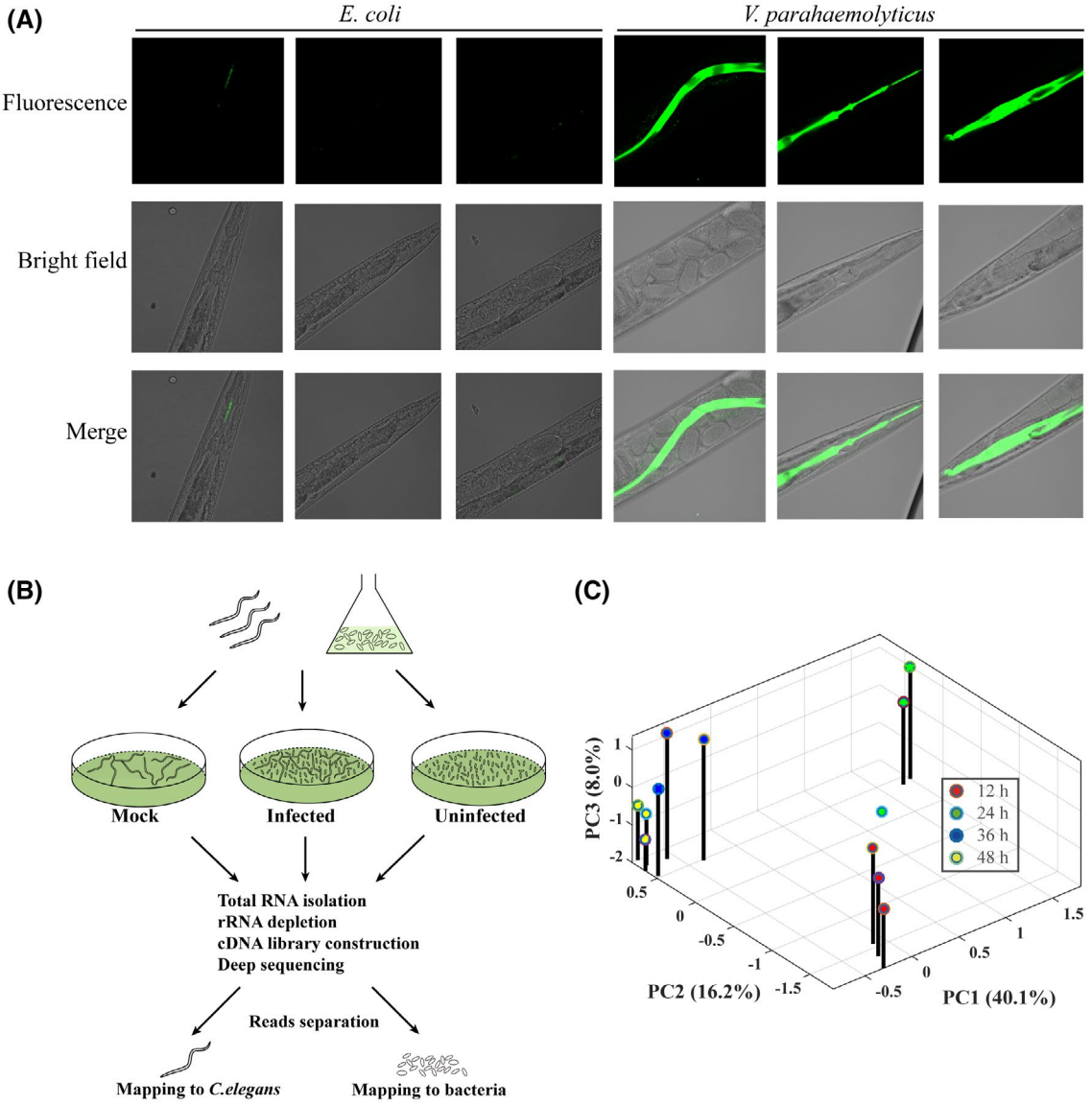

FIGURE 1 Establishment of an organism dual RNA-Seq with *C. elegans* and *V. parahaemolyticus*. A, *V. parahaemolyticus* successfully colonizes in the intestine of *C. elegans*. *E. coli* OP50 or *V. parahaemolyticus* RIMD2210633 expressing GFP was mixed with *C. elegans*. The worms were observed under fluorescent microscopy at 24 hours post infection. B, The workflow of organism dual RNA-Seq. L4 *C. elegans* were infected with *V. parahaemolyticus* (infected) or with *E. coli* OP50 (mock). *V. parahaemolyticus* grown in the medium (uninfected) was used as the bacterial control. Every sample was grown in the same medium and under the same environmental condition. C, Principal component analysis (PCA) of mean centered and scaled rlog-transformed read count valued of infected sample of RNA-Seq data

3 | RESULTS AND DISCUSSION

3.1 | Establishment of an organism dual RNA-Seq with *V. parahaemolyticus* infected *C. elegans*

In our attempt to investigate the infection mechanism of *V. parahaemolyticus*, we chose *C. elegans* as an infection model, which was previously shown to be susceptible to pathogenic *V. parahaemolyticus*.[39] Upon mixing with serotype O3:K6 strain RIMD2210633 in a liquid broth, *C. elegans* began to die from 48 hours post infection, and only 40% animal survived at 96 hours post mixing. In contrast, none of *C. elegans* died during this period of time when *E. coli* OP50 were mixed with the animals (Figure S1A). To examine whether the death of *C. elegans* attributed to a successful bacterial accumulation in the animal intestine, *C. elegans* were infected by GFP-tagged *E. coli* and *V. parahaemolyticus,* respectively, and bacterial colonization was examined with fluorescence microscopy (Figure 1A). *V. parahaemolyticus* successfully colonized in *C. elegans* as demonstrated by strong green fluorescence. A quantification of *V. parahaemolyticus* by CFU enumeration showed a ~10^6 bacteria per worm in average at this time point. In contrast, only weak fluorescence

was detected in animals infected with GFP-tagged *E. coli*, corresponding to above 4-log fewer bacteria recovered from the worm. Though colonization of *E. coli* was increased after 24 hours, the number of *V. parahaemolyticus* recovered from worm consistently has about 2-log higher than that of *E. coli* (Figure S1B). Our results together suggested that *V. parahaemolyticus* RIMD2210633 is pathogenic to *C. elegans*, which is feasible to be used as an infection model to investigate *V. parahaemolyticus* infection by dual RNA-Seq study.

We next established an organism dual RNA-Seq using *V. parahaemolyticus* infected *C. elegans*. Animals infected with bacteria were collected at 12, 24, 36, and 48 hours post infection, and the total RNA was extracted. Subsequently strand-specific Illumina-based deep sequencing were performed and the reads were matched to the genome of *C. elegans* or *V. parahaemolyticus* RIMD2210633, respectively (Figure 1B). More than 39 million reads in total were obtained from each infected sample, among which over 87% to 97% were mapped to the worm genome and ~0.025% to 3.4% to the bacterial genome (Dataset S1). For the cDNA libraries of each mock *C. elegans* sample, at least 30 million reads were generated, more than 89% of which were mapped to *C. elegans* genome (Dataset S1). Furthermore, above 3 million reads were generated for each uninfected bacterial sample and nearly 86% were mapped to *V. parahaemolyticus* genome (Dataset S1). Host and pathogen global gene expression profiles were distinct, and profiles of the three biological triplicates were clustered together (Figures 1C and S1C).

3.2 | Reprogramming of *V. parahaemolyticus* transcriptome during infection

3.2.1 | Untargeted analysis of *V. parahaemolyticus* transcriptome data

To identify the alterations in infection-specific gene expression, which subsequently could lead to the precise adjustment of virulence and fitness programs of the pathogen, we profiled the entire transcriptional landscape of *V. parahaemolyticus* grown under laboratory conditions (in vitro) and at different time point during colonization in *C. elegans* (in vivo) (Figure 1B). Using Deseq2 program, genes with different expression ($\log2fc > 1$; $\log2fc < -1$; adjusted $P < .05$) were identified at all four infection time points, with a total number between 1100 and 1800, corresponding to half of the genome of *V. parahaemolyticus*. Bacteria seem quickly adjust the gene expression profile during infection, as only a core set of 229 transcripts being common to all four time points of infection (Figure 2A, Dataset S2).

We analysed the dynamic transcriptome changes in *V. parahaemolyticus* during *C. elegans* infection, and a total of 1320 altered transcripts in bacteria upon *C. elegans* infection were hierarchically grouped into six clusters based on their expression patterns (Figure 2B, Dataset S2). Genes in cluster 1 were highly induced from 12 to 48 hours and were enriched in the amino acids transportation and metabolism as well as transcription based on their COG term functions (Figures 2B and S2A, B, Dataset S2), indicating that bacteria need to adjust their transcription profile as well as subsequent protein synthesis to overcome the challenge from the hostile environment and facilitate their infections. When the genes in cluster 1 were subject to KEGG annotation, of 32 genes that have been annotated, 12 genes were highly upregulated and associated with amino acid synthesis (Dataset S2). The upregulations on genes for amino acid synthesis might lead to subsequent increased protein synthesis. Indeed, the expression of ribosome proteins and genes involved in post-translational modification were highly induced at 24 and 36 hours post infection, respectively (Figure S2A, B, Dataset S2). In contrast to cluster 1, genes in cluster 6 were mostly repressed during the whole infection process and a significant part of these genes are involved in signal transduction (Figures 2B and S2A, B, Dataset S2).

The remaining four clusters have different dynamic transcriptome changes compared to cluster 1 and 6. Genes in cluster 2, 3, and 4 were repressed or demonstrated no change at the early infection time points, but were significantly induced at the late stage (Figure 2B). Genes in cluster 4 were highly induced after 36 hours post infection and were enriched in cell motility (Figures 2B and S2A, B), indicating that bacterial movement was restricted during the initial infection period. In sharp contrast, genes in cluster 5, which contains the majority of genes with altered expression profiles, were induced at the early infection stage but subsequently repressed. Interestingly, the function of 68% genes in this cluster is unknown (Figure 2B, Dataset S2).

Genes in cluster 2 were induced after 12 hours post infection and were enriched in translation, cell cycle control and cell wall/membrane/envelope biogenesis, whereas those in cluster 3 were highly induced after 24 hours post infection and were enriched in energy production (Figures 2B and S2A, B). Examination on the transcripts related to energy production in cluster 3 found that genes encoding enzymes for fatty acid oxidation, glycolysis and subsequent TCA cycle were strongly induced from 24 hours post infection (Figure 2C, Dataset S2). In contrast, genes involved in anaerobic respiration were highly repressed. Interestingly, genes encoding proteins for the electric transport chain (ETC) (*vp2300*, *vp0443*, *ccoP,* and *atpC*) were also upregulated at 24 hours or 36 hours post infection (Dataset S2).

3.2.2 | Target analysis of *V. parahaemolyticus* transcriptomic profiles

Bacterial pathogens utilize a multitude of methods to invade mammalian hosts, thwarting the immune system from

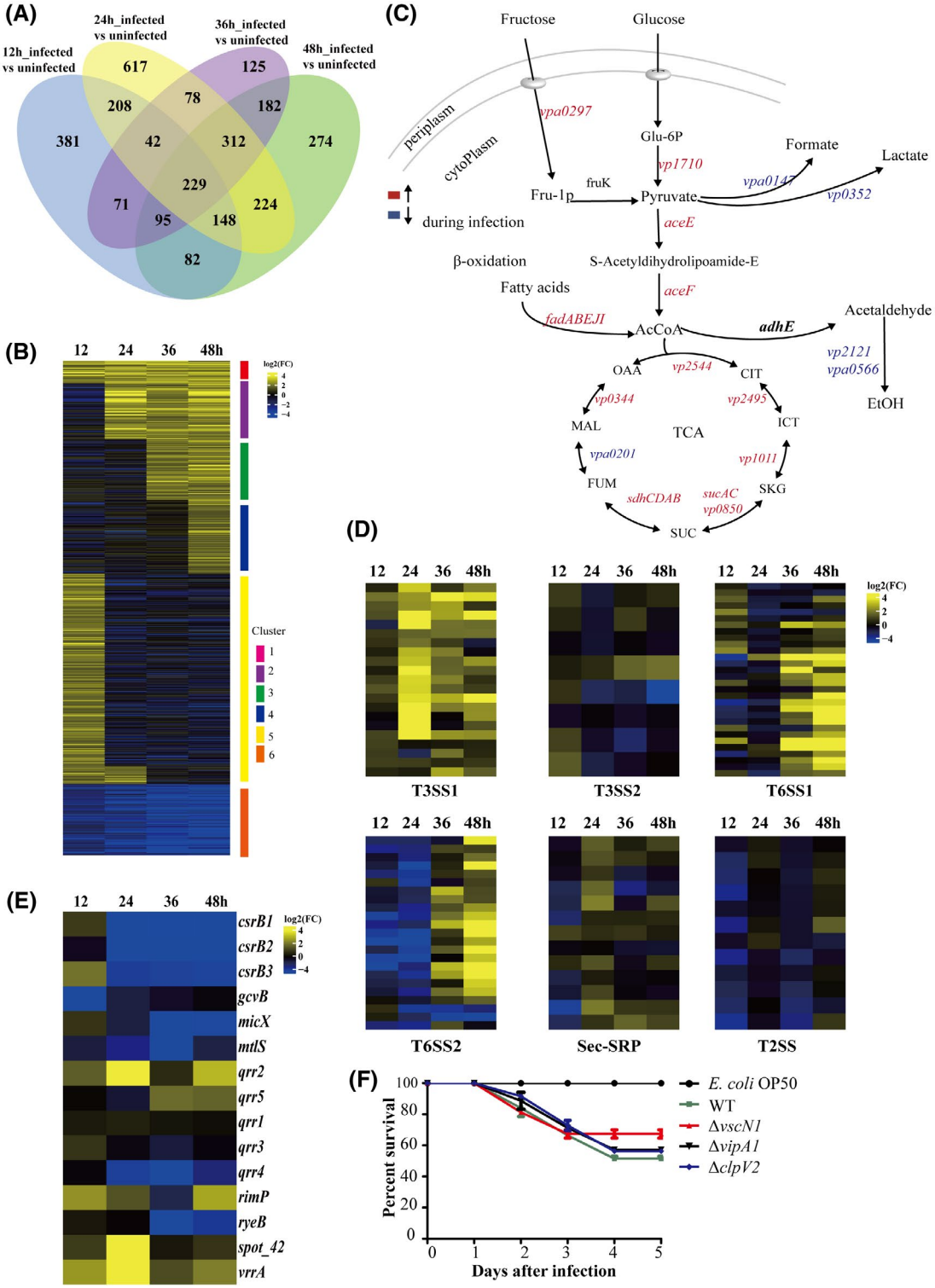

FIGURE 2 The transcriptional responses of *V. parahaemolyticus* during its infection to *C. elegans*. A, Venn diagram illustrating the number of differentially expressed genes (log2fc > 1; log2fc < −1; adjusted *P* value < .05) of *V. parahaemolyticus* across various time points post infection. B, Heat map of the *V. parahaemolyticus* transcripts during the whole infection time course. Enriched transcripts with increased level during infection are given in yellow, and transcripts with decreased level are indicated in blue. C, The altered expression in genes from central carbon metabolism of *V. parahaemolyticus*. Genes with enhanced expression at 36 hours post infection are indicated in red font, and those with decreased expression are indicated in blue. D, Differential expression of *V. parahaemolyticus* secretion systems in vivo compared to that in bacteria grown under in vitro condition. E, Heat map of transcripts of bacterial ncRNAs during infection to *C. elegans*. F, Mutations in T3SS1 or T6SSs compromised the virulence of *V. parahaemolyticus* to *C. elegans*

responding and damaging the infected tissue sites. Secretion systems are commonly used by pathogens to secrete virulence factors from the bacterial cytosol into host cells or the host environment to disrupt their functions and facilitate bacterial infections. *V. parahaemolyticus* encodes several secretion systems, including one general secretion pathway (Sec-SRP), one type II secretion system (T2SS), two T3SSs (T3SS1 and T3SS2), and two T6SSs. Both T3SSs are involved in the virulence toward mammalian cells.[12] The function of T6SSs are less studied but T6SS2 likely contribute to bacterial virulence.[12,22] Analysis on the transcription profile of different secretion systems found that T3SS1 was activated from 12 hours post infection, and consistently being induced throughout the whole infection process (Figure 2D, Dataset S2). The two T6SSs were initially repressed during the early infection but induced from 36 hours post infection, suggesting that T6SSs might also be involved in the infection to *C. elegans* (Figure 2D, Dataset S2). In contrast, the expression of genes in T2SS, and T3SS2 was not shown significant changes. Furthermore, the genes in Sec-SRP were slightly induced from 24 hours post infection (Figure 2D, Dataset S2).

Non-coding small RNAs (ncRNAs) are post-transcriptional regulatory molecules that fine-tune the important processes in bacterial physiology toward host infection. Analysis on the transcripts of *V. parahaemolyticus* colonized in *C. elegans* revealed that the expression of total 19 trans-encoded ncRNA was subject to changes compared to those in bacteria cultured in vitro, including the CsrB (carbon storage regulator B) and Qrr (quorum regulatory RNA) ncRNAs. CrsB family ncRNA is widespread among eubacteria and its members participate in many global regulators circuits.[40] *V. parahaemolyticus* contains three CsrBs and all of them were highly repressed during the *C. elegans* infection, especially 12 hours post infection (Figure 2E, Dataset S2). ncRNA Qrrs in many other bacteria, including *Vibrio cholerae*, not only regulate quorum sensing but also control the expression of virulence factors.[41,42] *V. parahaemolyticus* have 5 Qrrs with different expression patterns during infection: Qrr2 and Qrr5 were induced, whereas the expression of other three was either repressed (Qrr4) or unchanged (Qrr1 and Qrr3). The ncRNA VrrA of *V. parahaemolyticus* was upregulated during the whole infection process (Dataset S2). VrrA is the first ncRNA known to control outer membrane vesicle (OMV) formation, which has been suggested to promote the adherence, the transfer of bacterial DNA and the delivery of virulence factors to other bacteria or eukaryotic cells.[43,44] VrrA in *V cholerae* has been shown to affect virulence.[45] Therefore, the induction of VrrA (Figure 2E, Dataset S2) could also have an important role in bacterial pathogenesis or contribute to the survival of *V. parahaemolyticus* in *C. elegans*.

Two-component regulatory systems are commonly used by bacteria to sense and respond to their environments. *V. parahaemolyticus* experiences a different environment condition during the colonization in the intestine of *C. elegans*, which could be sensed by two-component system(s) to adjust its transcriptome profiles. Our analysis on the expression of two-component system found that *vpa1515* and *vpa0182* were repressed after 12 hours post infection (Dataset S3). In contrast, *vp2567*, a gene encoding a sensor homologous to BarA in *Pseudomonas syringae*, was significantly upregulated from 12 hours post infection (Dataset S3). The homologs of BarA (VP2567), together with its regulator UvrY (VP1945), has been found in a wide range of gram-negative bacteria and controls the production of secondary metabolites and extracellular enzymes involved in pathogenicity to plants and animals, ecological fitness, or tolerance to stress.[46] However, the function BarA/ UvrY system in *V. parahaemolyticus* is still unknown yet.

3.2.3 | Validation of transcriptional alteration and the identified potential virulent factors

The altered transcriptional profiles of selected genes were validated by RT-PCR. Consistent with the RNA-Seq results (Dataset S3), the expression of BarA was upregulated, whereas the expressions of *vpa0182* and *vpa1515* were repressed during the infection to *C. elegans* (Figure S3A). We also validated the induction of selected genes in TCA cycle and ETC chain and obtained similar results as observed in RNA-Seq analysis (Figure S3B-E). These verifications of RNA-Seq results by RT-PCR highlight the reliability of our organism dual RNA-Seq. The observation of the induction of TCA cycle and ETC chain are unexpected to us as the intestine of *C. elegans* is assumed to be a hypoxia environment, where the genes involved in TCA cycle or ETC are expected to be downregulated. The opposite observations indicate that *V. parahaemolyticus* might be able to use oxidative TCA cycle and alternative electron receptor for energy production during its infection to *C. elegans*. The use of oxidative TCA and alternative electron receptor under hypoxia environment is not unprecedent. In *Proteus mirabilis*, the TCA cycle was found to be utilized by anaerobic respiration.[47] In the gut of host, *Salmonella* uses tetrathionate as a terminal electron to produce a growth advantage over the competing microbiota.[48,49] It is possible that *V. parahaemolyticus* uses similar mechanisms to establish colonization in the intestine of the host. Alternatively, the hostile environment in *C. elegans* may decrease the membrane potential of *V. parahaemolyticus* as observed in *Pseudomonas aeruginosa*.[50] If so, bacteria may upregulate the expression of genes involved in TCA cycle and ETC as a feedback to compensate the decrease in ATP production.

We next examined whether the upregulation of secretion systems correlated with their roles in *V. parahaemolyticus* pathogenesis in the *C. elegans* model, we constructed in-frame deletion mutants in T3SS1 ATPases VscN1 (Δ*vp1668*), T6SS1 (Δ*vipA1*), T6SS2 (Δ*clpV2*), and test the virulence of mutants toward *C. elegans*. As shown in Figure 2F, defects in the function of either T3SS1, T6SS1, or T6SS2 significantly compromised the infection of *V. parahaemolyticus* to *C. elegans*, and the survival of animal infected by the mutants was increased about 5 to 20% compared to those infected by WT. These results suggest that both T6SSs and T3SS1 contribute to the pathogenesis of *V. parahaemolyticus* for their infections to the worms. Indeed, both T3SS1 and T6SS2 in *V. parahaemolyticus* were known to be virulence factors for mammalian host.[18,22] Thus, our results suggest that *C. elegans* is a good animal model to study the pathogenesis of *V. parahaemolyticus* by organism dual RNA-Seq, which can help discover bacterial virulence factors to mammalian host.

3.3 | Host transcriptional responses to *V. parahaemolyticus* infection

The host gene expression profile was generated by the differential expression analysis package DESeq2, and genes showing statistically significant changes in the expression level by at least 1.5-fold (adjusted $P < .05$) were considered (Dataset S4). To figure out the counter response of *C. elegans* to *V. parahaemolyticus* infection, of the 46 739 profiled host transcripts, 2136 were screened out based on genes expression alterations in *C. elegans* infected by *V. parahaemolyticus* compared to those uninfected (Figure 3A). These transcripts were subsequently grouped into three clusters: transcripts in cluster 1 (Dataset S4) are consistently upregulated; transcripts in cluster 2 (Dataset S4) were induced 12 hours or 24 hours post infection; whereas genes in cluster 3 (Dataset S4) are repressed during all the four infection time points (Figure 3A). The elevated gene expression of selected genes from cluster

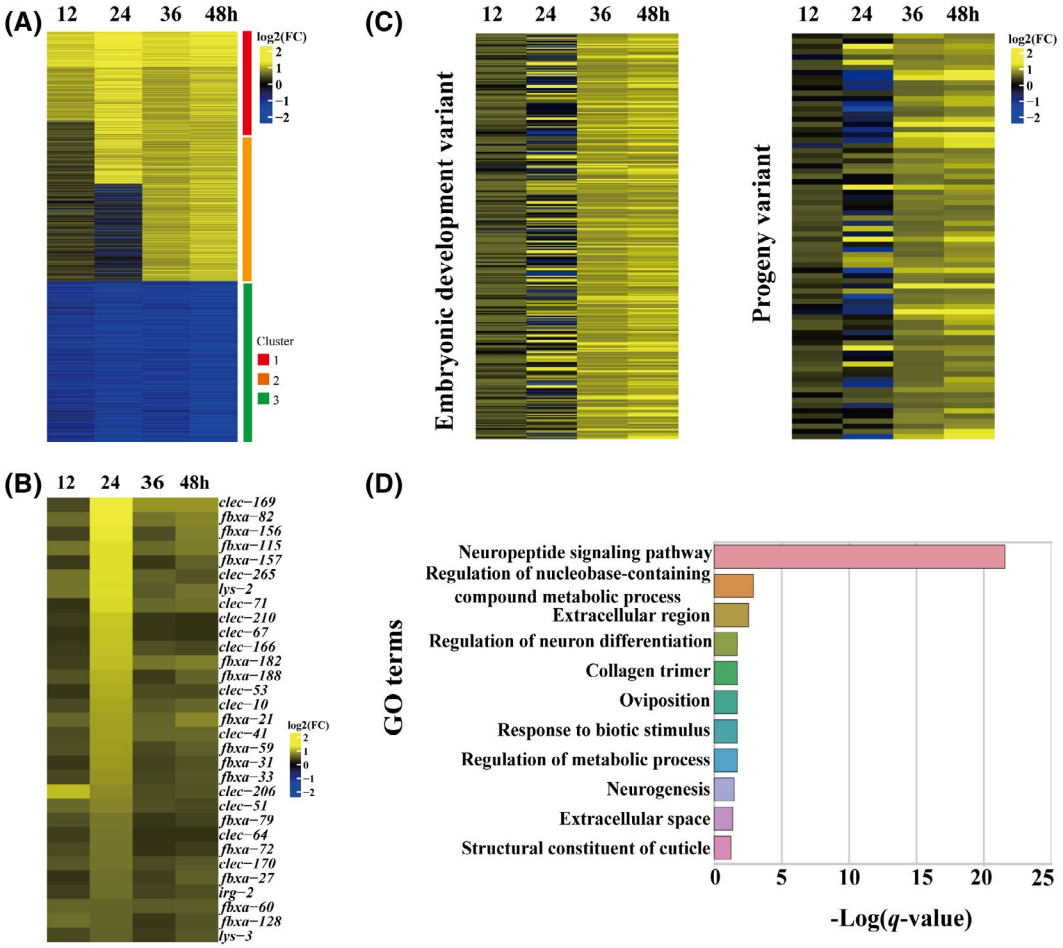

FIGURE 3 *V. parahaemolyticus* infection induces rapid alterations in host gene expression. A, Heat map of *C. elegans* transcripts during the whole infection course. The transcripts with a cutoff of −1.5 > FC > 1.5 are included for analysis. Enriched transcripts during infection are given in yellow, and decreased transcripts are indicated in blue. B, Heat map of highly enriched immunity effectors in *C. elegans* during *V. parahaemolyticus* infection. C, Heat map of genes in the mostly enriched phenotype terms from cluster 2. D, The most significant Gene Ontology (GO) term of genes from cluster 3 of Figure 3A

1 and cluster 2 was verified by qRT-PCR (Figure S4A, B), confirming the validity of our dual RNA-Seq results.

To investigate whether genes with the similar expression pattern were enriched in any specific pathway or potentially influence any phenotype on *C. elegans*, we analysed genes in each cluster using TEA (Tissue), PEA (Phenotype) and GEA (Gene Ontology [GO]) enrichment methods. The majority (62%) of genes in cluster 1 are specifically expressed in cells from intestine by TEA analysis (Figure S4C, Dataset S4), and 483 genes in this cluster can be further enriched in 15 GO terms (Dataset S4). The most highly enriched GO term, with 60 genes demonstrating the most significantly altered transcriptions from this cluster, associates with the immune system process (Figure S4D). In addition, 10 genes are involved in the response to biotic stimulus. Manual examination on the genes in these enriched two GO terms found that they are specifically expressed in the intestine cells, suggesting that there was a strong immune response to *V. parahaemolyticus* infection in the worm gut (Figure S2B). Of the 60 genes associated with the immune system process, 42 were well annotated in NCBI. The encoding protein of these genes include (Figure 3B, Dataset S4): (i) C-type lectins (such as CLEC-10, CLEC-40, and CLEC-170), a family of surface receptors known to recognize microbial carbohydrate moieties, which can sense products from dying cells and transduce inflammatory signals that modulate the immune system[51]; (ii) F-box A protein (FBXA-20, FBXA-59, FBXA-60, FBXA-82, and FBXA-156), one family proteins with F-box motif that involves in ubiquitin-mediated proteolysis, which function as the key regulator in many pathways of cell signalling, transcription, and cell division[52]; (iii) Lysozymes. In *C. elegans*, there are ten genes encoding lysozymes for antimicrobial proteins against bacteria.[53] Our results showed that most of lysozymes in *C. elegans* were induced at different time point post infection, and LYS-2 and LYS-3 were consistently induced throughout the infection process (Figure 3B, Dataset S4).

The transcripts in cluster 2 are induced only from 12 to 24 hours post infection, and 80% of those genes are enriched in reproductive system by TEA (Dataset S4). Of the 822 genes in this cluster, 88 are associated with the GO terms of meiotic cell cycle and embryo development ending in birth or egg hatching (Figure S4E, Dataset S4), suggesting that *V parahaemolyticus* infection might affect the reproduction of *C. elegans*. The enrichment of genes in reproductive system could also reflect the development of *C. elegans* from L4 stage to adult, as elevated expression level in the genes related to gonad development was observed during the time course of 48 hours in our experiment (Figure S4F). However, we also noticed higher expression level of these genes in the *C. elegans* infected by *V. parahaemolyticus*, suggesting the reproduction of *C. elegans* during *V. parahaemolyticus* infection is likely affected. PEA analysis showed that the elevated expression of genes in cluster 2 could cause different variants in *C. elegans* from 12 hours post infection (Figure S2B), including embryonic development variant and progeny variant (Figure 3C, Dataset S4). Examination on the genes in this cluster found that the elevation of certain genes could repress the variant formation in *C. elegans*. For example, SMO family genes play important role in repairing DNA damage,[54] SMO-1 modification on the ubiquitin E3 HERC2 triggers recruitment of further repair factors at DNA repair foci, including the ubiquitin E3 BRCA1/BARD1[55]; POS-1 has an important role in regulating the expression of maternal mRNAs in germline blastomeres, and mutations in *pos-1* cause several defects in the development of the germline blastomeres[56]; PUF RNA-binding proteins (RNABPs), PUF-3/11 and PUF-5/6/7, control different specific aspects of oocyte formation: silencing PUF-3/-11 via RNAi yielded an embryonic lethal phenotype,[57] whereas depletion of PUF-5 and PUF-6/7 together caused defects in oocyte formation and early embryonic cell divisions.[58] Our results suggest that DNA damage might occur in the reproduction system of *C. elegans* during bacterial infection. Germline DNA damage was shown to activate the systemic immune response, such as the UPS (ubiquitin proteasome system), and induce the expression of host defense effectors.[59] Consistently, we observed that genes in UPS were upregulated (Dataset S4).

Genes in cluster 3 are highly repressed throughout the bacterial infection process (Figure 3A). Of those 831 genes in this cluster, 65% have not been annotated for their functions (Dataset S4). However, TEA showed that genes for nervous system were only enriched, implying that nervous system was affected by *V. parahaemolyticus* infection (Figure S2B, Dataset S4). The PEA analysis suggests that *V. parahaemolyticus* might affect *C. elegans* movement (Dataset S4). Indeed, we observed that *C. elegans* was less active when seeded on *V. parahaemolyticus* lawn compared to those on *E. coli* OP50.

GEA analysis showed that cluster 3 genes are most possible enrichment in neuropeptide signaling pathway (Figure 3D, Dataset S4), which indicating that signaling pathway of *C. elegans* may be affected by *V. parahaemolyticus*. There are three main signal pathways that are important for innate immunity response in *C. elegans*[60]: MAP kinase-mediated signaling cascades, insulin-like signaling pathway, and non-conventional signaling pathway. The crucial genes in non-conventional signaling pathway, *mpk-1*, the product of which can activate the UPS system, were induced during *V. parahaemolyticus* infection.[61] Consistently, genes in UPS system were found being upregulated and enriched in cluster 1 (Figure 3A, B). In contrast, genes in MAP kinase-mediated signaling cascades, enriched in cluster 3, were significantly repressed upon *V. parahaemolyticus* infection (Dataset S4): the expression of *tir-1* and its downstream genes, such as *nlp-29* and *nlp-31*, as well as the genes involved in MAP kinase-related signaling pathway, such as *nsy-1* and *sek-1*, were decreased during infection (Dataset S4). MAP kinase-related

signaling pathway is an essential player in antimicrobial defense.[62] This MAP kinase-related signalingpathway is orthologous to the mammalian apoptosis signal-regulating kinase 1 (ASK1) - MAPK kinase 3/6 (MKK3/6) - p38 MAPK cascade, which is also involved in triggering innate immune responses. Knock-down of *tir-1* in *C. elegans* abolished the activation of MAP kinase-related signaling pathway.[63] The observation of downregulation of MAP kinase-mediated signaling cascades suggests that *V. parahaemolyticus* might repress host innate immunity pathway for better survival. We did not observe significant transcript changes in genes for insulin-like signaling pathway (such as *daf-16*, *skn-1*) (Dataset S4).

3.4 | Importance of BarA/UvrY for modulating host transcriptional responses

Innate immunity is the first line defense of host to control microbial infection. In *C. elegans*, several defense effectors have been reported, such as defensin (ABF-2), saponin (SPP-1), and several others with homology to antimicrobial proteins: lysozymes (LYS-1 to LYS-10), thaumatin-like protein (THN), and a CUB-domain containing protein, F08G5.6.[64] Upon infection by *Salmonella typhimurium*, the expression of *abf-2* and *spp-1* in *C. elegans* was highly induced.[65] Similarly, *thn-2* were also upregulated upon the infection by *Enterococcus faecalis* and *Microbacterium nematophilum*.[66] Interestingly, we found that the expression of *spp-1*, *thn-2,* and *abf-2* were significantly repressed after 24 hours post *V. parahaemolyticus* infection (Figure S5A, Dataset S4). The downregulation of these genes was further confirmed by qRT-PCR analysis (Figures 4A and S5B). In addition, the genes involved in MAP kinase signaling pathway were also downregulated (Figures 4B and S5C, Dataset S4).

Two-component system plays important role to sense and respond to their environmental changes, especially during host infection. We investigated the contribution of BarA/UvrY in *C. elegans* infection as the expression of BarA was enhanced upon the infection process. We then hypothesize that BarA/UvrY might contribute to the decreased expression

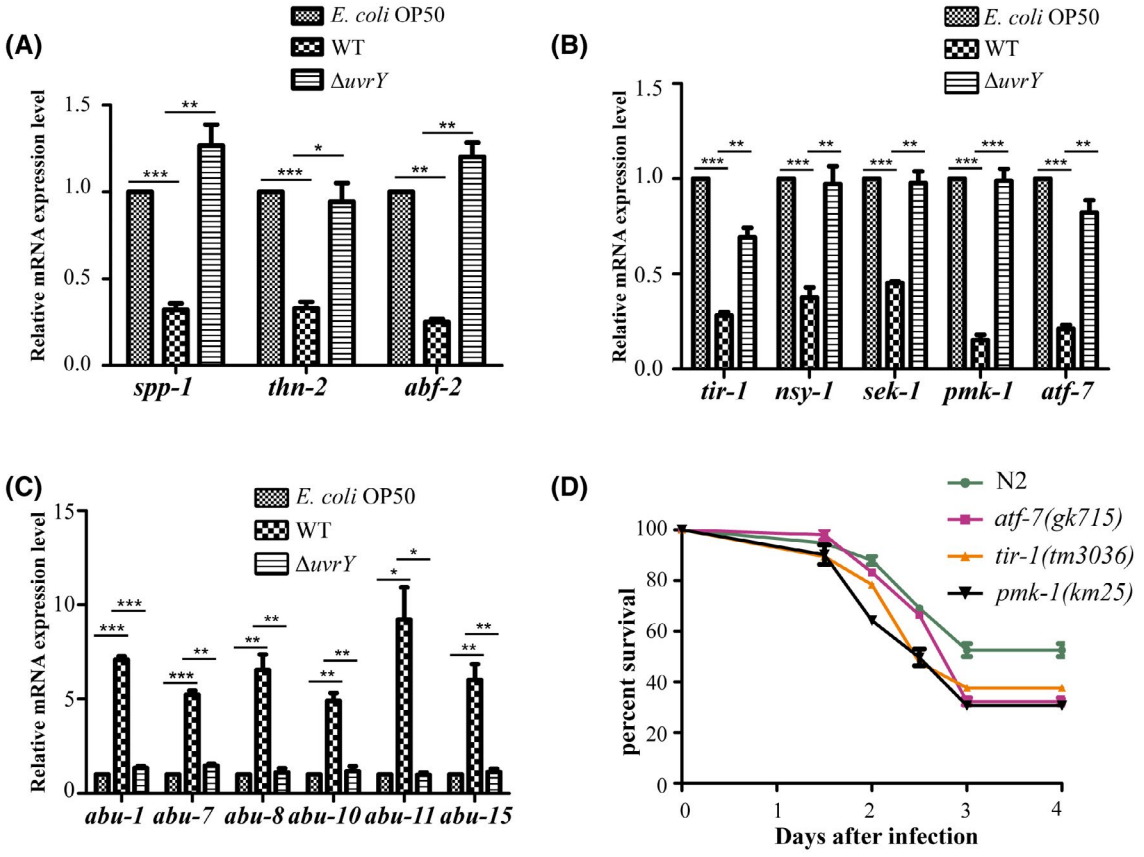

FIGURE 4 BarA/UvrY regulates host immune response. A, The expression of *spp-1, thn-2* and *abf-2* in WT worms exposed to *E. coli* OP50 or *V. parahaemolyticus*. B, The expression of selected genes from MAP kinase signaling pathway in the *C. elegans* exposed to *E. coli* OP50 or *V. parahaemolyticus*. C, *V. parahaemolyticus* infection triggers the upregulation of genes associated with ER stress response. For (A), (B) and (C), the expression of genes was examined by qRT-PCR analysis in the *C. elegans* exposed to *E. coli* OP50 or *V. parahaemolyticus* at 48 hours post infection. Results indicate mean ± SD of four replicates from two independent experiments. P values were determined by paired t test (*$P < .05$; **$P < .01$; *** $P < .001$). D, Innate immunity factors in *C. elegans* contribute to the defense against *V. parahaemolyticus* infection. Mutations in selected innate immunity factors result in decreased survival of *C. elegans* against the infection by *V. parahaemolyticus*

level of the abovementioned genes. In-frame deletion mutant of *uvrY* was constructed. We infected *C. elegans* by *V. parahaemolyticus* WT or Δ*uvrY* and compared the expression of genes in MAP kinase signaling pathway by qRT-PCR at 24 and 48 hours post infection. Our results showed that the expression level of *tir-1, nsy-1*, *sek-1*, *pmk-1*, and *atf-7* in *C. elegans* infected by Δ*uvrY* was increased to a similar level as those in worms seeded on *E. coli*, and was significantly higher than those in worms infected by WT (Figures 4B and S5C). In contrast, the expression of *abu-1*, *abu-7*, *abu-8*, *abu-10*, *abu-11,abu-14, abu-12,* and *abu-15* in worms, which play a role in infection tolerance,[67] were highly induced upon the infection by WT but not Δ*uvrY* (Figures 4C and S5D). These results suggest *V. parahaemolyticus* represses selected immunity factors during its infection. *V. parahaemolyticus* was previously shown to either activate or repress p38-MAPK pathway by different effectors of T3SS in distinct mammalian cell lines.[63,68,69] Our study on bacteria-host interaction at organism level likely imply the comprehensive effect of *V. parahaemolyticus* on MAP kinase pathway during its infection.

To examine whether the repressed immunity factors are important for worm to control bacterial infection, *V. parahaemolyticus* was used to infect *C. elegans* WT or *tir-1*, *pmk-1, atf-7* animals, and the survival of worm was examined. Animals defect in *tir-1(tm3036)*, *pmk-1(km25)*, and *atf-7(gk715)* exhibited enhanced susceptibility to *V. parahaemolyticus* infection (Figure 4D), which is consistent with the previous study result.[39,70,71] Our results suggest that *V. parahaemolyticus* inhibits the host innate immunity in *C. elegans* via downregulation of MAP kinase pathways much as it does in mammalian cell

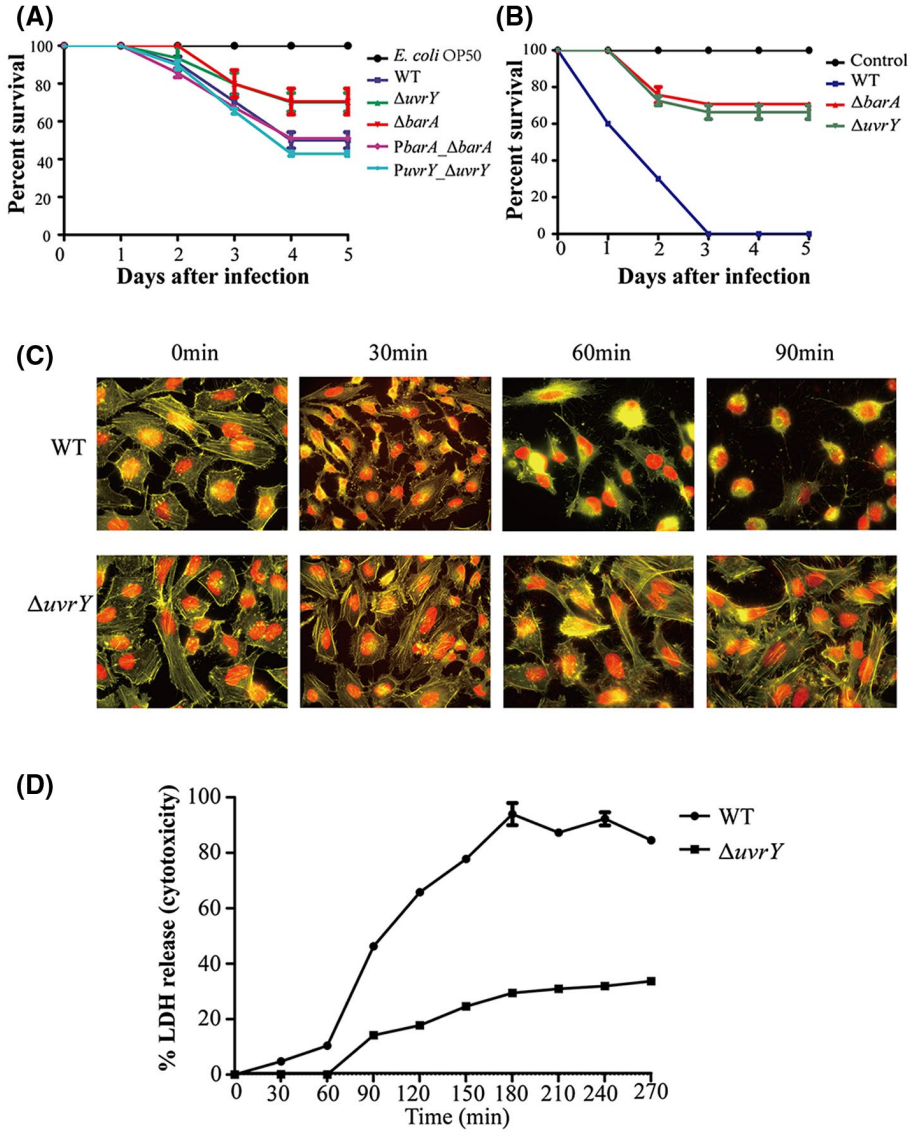

FIGURE 5 BarA/UvrY contributes to *V. parahaemolyticus* pathogenesis. A, Deletion of *barA* or *uvrY* resulted in increased survival of *C. elegans*. B, Δ*barA* and Δ*uvrY* are highly attenuated in a Zebrafish model. C, Deletion of *uvrY* compromised bacterial virulence toward HeLa cells. Cells were examined by fluorescent microscopy. The DNA and actin of HeLa cells were stained by Hoechst (red) and phalloidin (yellow), respectively. D, Cytotoxicity of *V. parahaemolyticus* to Hela cells examined by lactate dehydrogenase (LDH) assay

lines.[72,73] However, our current results could not differentiate whether the repression of these immunity factors could enhance the colonization of *V. parahaemolyticus* in *C. elegans* or bacterial toxicity to the host, which warrant further study.

3.5 | Importance of BarA/UvrY for virulence of *V. parahaemolyticus*

To demonstrate the contribution of BarA/UvrY to the virulence of *V. parahaemolyticus*, Δ*barA* and Δ*uvrY* were used to infect *C. elegans* and the survival of *C. elegans* was investigated. Our results demonstrated that the survival of *C. elegans* infected with Δ*barA* and Δ*uvrY* were significantly improved by 20 to 30% compared to those infected by WT (Figure 5A). The decrease in virulence of Δ*barA* or Δ*uvrY* toward *C. elegans* was fully recovered by a complementation of the WT copy of individual gene *in trans*. Importantly, in a Zebrafish model, a similar attenuation was also observed for both Δ*barA* and Δ*uvrY* (Figure 5B). *V. parahaemolyticus* was previously shown to induce cell rounding and rupture in HeLa cell,[74] we tested whether deletion of *barA/uvrY*

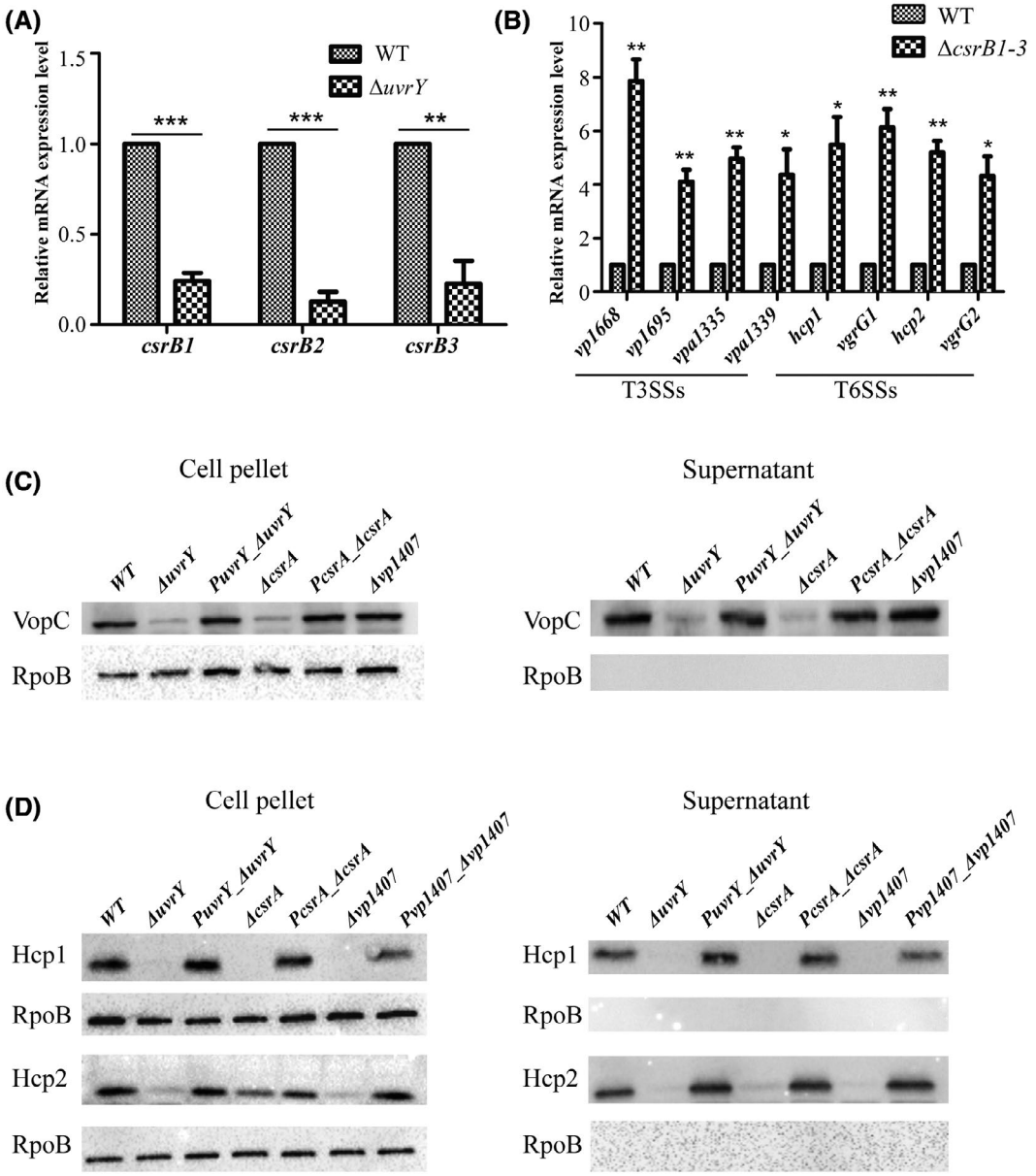

FIGURE 6 UvrY controls T3SSs and T6SSs through VP1407 and Csr system. A, CrsBs were controlled by UvrY. The expression of CsrBs genes in WT strain and Δ*uvrY* was analyzed by qRT-PCR analysis. B, CsrBs controls T3SSs and T6SSs. The expression of selected genes from T3SSs and T6SSs in the triple deletion mutant of *csrB1-3* was analyzed by qRT-PCR analysis. For (A) and (B), results indicate mean ± SD of four replicates from two independent experiments. P values were determined by paired t test (*$P < .05$; **$P < .01$; *** $P < .001$). C, Western blot analysis of VopC expression and secretion in various mutants. RpoB was used as the loading control. D, Western blot analysis of the expression and secretion of Hcp1 and Hcp2 in various mutants. RpoB was used as the loading control

compromised the bacterial virulence in these cells. As shown in Figure 5C, *V. parahaemolyticus* WT caused significant cytotoxicity to HeLa cells from 60 minutes post infection: HeLa cells were detached, became round and eventually died. In contrast, most HeLa cells infected with Δ*uvrY* spread properly in the dish and less cells were detached. A quantification showed that only about 30% HeLa cells infected by Δ*uvrY* mutant died at 270 minutes post infection, in contrast to near 100% HeLa cells died at the same time point (Figure 5D). Taken together, our results demonstrated that the two-component system BarA/UvrY is an important virulence factor in *V. parahaemolyticus*.

3.6 | The regulation of BarA/UvrY on T3SSs and T6SSs

As T3SSs are critical virulence factors in *V. parahaemolyticus*, we examined whether T3SSs are under the control of BarA/UvrY, and T6SSs were also included for analysis. Our results showed that deletion of *uvrY* or *barA* compromised the expression of selected genes from both two T3SSs and two T6SSs by 2 to 10-fold at 23°C (Figure S6A, B). Furthermore, Western blot analysis showed that the expression and secretion of effectors from T3SS2 (VopC),[34] T6SS1 (Hcp1), and T6SS2 (Hcp2)[75] were significantly decreased in Δ*uvrY*, and these defects were fully recovered by a complementation of Δ*uvrY* with WT copy of *uvrY* (Figure 6C, D).

We next investigated the direct target of UvrY in *V. parahaemolyticus* by ChIP-Seq with a chromosomally encoded 3 × FLAG-tagged UvrY (Dataset S1). A ChIP-qPCR confirmed by examination of the selected candidates from ChIP-Seq that UvrY at least binds to the promoter regions of three ncRNA (CsrB1, CsrB2, and CsrB3), the gene of T3SS1 regulator VP1698, and the gene of potential T6SS1 regulator VP1407 (Figure S7A, Dataset S1).

Carbon storage regulator family ncRNA represents a conserved regulator that plays important role in regulating the bacterial physiology in many other bacteria.[76] Deletion of *uvrY* significantly reduced CsrB expression level in vitro when bacteria were cultured in LB medium at 23℃, suggesting that UvrY positively control CrsBs in vitro (Figure 6A). Furthermore, simultaneous deletion of all three CrsB ncRNA significantly increased the expression level of genes in both T3SSs and T6SSs, indicating that CsrB negatively regulates T3SSs and T6SSs (Figure 6B). CsrA is one inhibitory target of CsrBs in many bacteria.[77-79] Consistently, deletion of *csrA* dramatically reduced the expression level of T3SSs and T6SSs as examined by qRT-PCR or Western blot analysis (Figures 6C, D and S7B), suggesting a negative regulatory cascade of T6SS/T3SSs by CsrB through CrsA. Interestingly, the expression levels of CsrBs were decreased in Δ*uvrY* under the in vitro condition (Figure 6A). In contrast, CsrBs were repressed during *C. elegans* infection, where BarA was induced (Figure S3A, Dataset S3). These results suggest that the regulation circuit during in vivo infection is more complicated than in vitro condition. Indeed, CrsBs are regulated by many factors in other bacteria.[80] Furthermore, though UvrY binds to promoter region of *vp1698*, the negative regulator of T3SS1, we did not find significant changes on the expression level of *vp1698* in Δ*uvrY* under in vitro condition (Figure S7C).

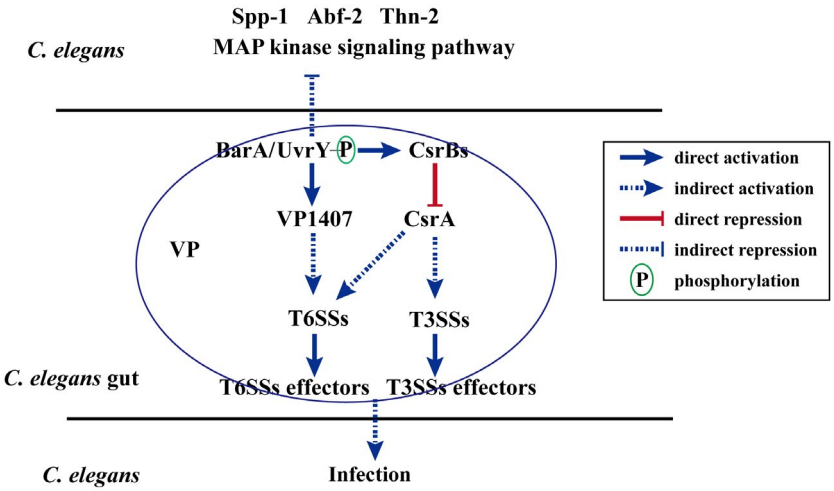

FIGURE 7 A model of the cross-talk between *V. parahaemolyticus* and *C. elegans* during the infection. After entering the host, the bacterial two-component system BarA/UvrY activates the secretion systems (both T3SSs and T6SSs) through the regulating Csr system and regulator VP1407. The secretion systems contribute to the successful infection of *V. parahaemolyticus* by secreting/translocating putative effectors. In addition, unknown virulence factor(s) controlled by BarA/UvrY represses host immunity effectors Spp-1, Abf-2, Thn-2, and the MAP kinase signalling pathway, which further facilitates bacterial infection

UvrY binds to the promoter region of *vp1407*, a gene predicted to encode a transcriptional regulator immediately downstream of type VI gene *vp1408* (Figure S7A). Deletion of *uvrY* compromised the expression of *vp1407* by at least 2.5-fold (Figure S7C). We hypothesized that VP1407 is a positive regulator controlling T6SSs. Indeed, the expression of selected genes, including *clpV* and *vgrG*, from T6SSs was significantly decreased in Δ*vp1407* as examined by qRT-PCR (Figure S7D), which is consistent with the reduced level of Hcp1 and Hcp2 in both bacterial pellet and the corresponding supernatant (Figure 6C, D), suggesting that UvrY controls both T6SS1 and T6SS2 through VP1407.

In summary, we have successfully established an organism dual RNA-Seq with *C. elegans* as a host model. Our studies with this technology on the interaction between pathogenic *V. parahaemolyticus* and *C. elegans* have provided the snapshots of the dynamic reorganization of cell transcriptions at organism level during the infections (Figure S2B). The analysis on the gene alterations have revealed insights into the cross-talk between pathogen and *C. elegans* host at the organism level (Figure 7). We discovered a number of virulence factors used by *V. parahaemolyticus*, including T3SS1 that has been shown to contribute to bacterial pathogenesis in mammalian host. In addition, we also identified that the two-component system BarA/UvrY plays a critical role for the pathogenesis in *V. parahaemolyticus*: it controls T3SSs and T6SSs though a regulatory cascade including the ncRNA CrsB/CsrA system. Importantly, our organism dual RNA-Seq analysis revealed that *V. parahaemolyticus* represses the innate immunity of *C. elegans* host during its infection through BarA/UvrY, demonstrating that our organism dual RNA-Seq is a powerful tool to define the host-pathogen cross-talk at organism level.

ACKNOWLEDGMENTS

We thank Prof. Garry Wong from Faculty of Health Sciences, University of Macau, for his critical review and comments. We acknowledge the Research Committee of the University of Macau (Grant No.: MYRG2016-00073-FHS, MYRG2016-00199-FHS and MYRG2019-000050-FHS) and the Macau Science and Technology Development Fund (Grant No.: FDCT/066/2015/A2, FDCT/0058/2018/A2 and FDCT/0113/2019/A2) for providing financial support for this research. Some strains of *C. elegans* were provided by the CGC, which is funded by NIH Office of Research Infrastructure Programs (P40 OD010440).

ETHICS STATEMENT

All zebrafish experiments were approved and performed according to the rules and regulations of the Panel on Research Ethics of University of Macau (UMARE-034-2016).

CONFLICT OF INTEREST

All authors declare no conflict of interest.

AUTHOR CONTRIBUTIONS

J. Zheng coined the concept; W. Zhang and J. Zheng designed the research experiments. W. Zhang conducted the experiment work; W. Zhang, R. Xie, and J. Zheng analysed the data; W. Zhang, X.D. Zhang, L.T.O. Lee, H. Zhang, B. Peng, and J. Zheng wrote the paper. M. Yang contributed reagent.

REFERENCES

1. Cloney R. Microbial genetics: dual RNA-seq for host-pathogen transcriptomics. *Nat Rev Genet*. 2016;17:126-127.
2. Wolf T, Kammer P, Brunke S, Linde J. Two's company: studying interspecies relationships with dual RNA-seq. *Curr Opin Microbiol*. 2018;42:7-12.
3. Westermann AJ, Barquist L, Vogel J. Resolving host-pathogen interactions by dual RNA-seq. *PLoS Pathog*. 2017;13:e1006033.
4. Saliba A-E, C Santos S, Vogel J. New RNA-seq approaches for the study of bacterial pathogens. *Curr Opin Microbiol*. 2017;35:78-87.
5. Westermann AJ, Gorski SA, Vogel J. Dual RNA-seq of pathogen and host. *Nat Rev Microbiol*. 2012;10:618-630.
6. Westermann AJ, Forstner KU, Amman F, et al. Dual RNA-seq unveils noncoding RNA functions in host-pathogen interactions. *Nature*. 2016;529:496-501.
7. Damron FH, Oglesby-Sherrouse AG, Wilks A, Barbier M. Dual-seq transcriptomics reveals the battle for iron during *Pseudomonas aeruginosa* acute murine pneumonia. *Sci Rep*. 2016;6:39172.
8. Aprianto R, Slager J, Holsappel S, Veening JW. Time-resolved dual RNA-seq reveals extensive rewiring of lung epithelial and pneumococcal transcriptomes during early infection. *Genome Biol*. 2016;17:198.
9. Baddal B, Muzzi A, Censini S, et al. Dual RNA-seq of nontypeable haemophilus influenzae and host cell transcriptomes reveals novel insights into host-pathogen cross talk. *mBio*. 2015;6:e01765-15.
10. Dhakal BK, Lee W, Kim YR, Choy HE, Ahnn J, Rhee JH. *Caenorhabditis elegans* as a simple model host for *Vibrio vulnificus* infection. *Biochem Biophys Res Commun*. 2006;346:751-757.
11. Vaitkevicius K, Lindmark B, Ou G, et al. A Vibrio cholerae protease needed for killing of *Caenorhabditis elegans* has a role in protection from natural predator grazing. *Proc Natl Acad Sci U S A*. 2006;103:9280-9285.
12. Letchumanan V, Chan KG, Lee LH. Vibrio parahaemolyticus: a review on the pathogenesis, prevalence, and advance molecular identification techniques. *Front Microbiol*. 2014;5:705.
13. Zhang L, Orth K. Virulence determinants for *Vibrio parahaemolyticus* infection. *Curr Opin Microbiol*. 2013;16:70-77.
14. Shimohata T, Takahashi A. Diarrhea induced by infection of *Vibrio parahaemolyticus*. *J Med Invest*. 2010;57:179-182.
15. Krachler AM, Orth K. Functional characterization of the interaction between bacterial adhesin multivalent adhesion molecule 7 (MAM7) protein and its host cell ligands. *J Biol Chem*. 2011;286:38939-38947.
16. Raghunath P. Roles of thermostable direct hemolysin (TDH) and TDH-related hemolysin (TRH) in *Vibrio parahaemolyticus*. *Front Microbiol*. 2014;5:805.
17. Kishishita M, Matsuoka N, Kumagai K, Yamasaki S, Takeda Y, Nishibuchi M. Sequence variation in the thermostable direct hemolysin-related hemolysin (trh) gene of *Vibrio parahaemolyticus*. *Appl Environ Microbiol*. 1992;58:2449-2457.

18. Park KS, Ono T, Rokuda M, et al. Functional characterization of two type III secretion systems of *Vibrio parahaemolyticus*. *Infect Immun*. 2004;72:6659-6665.
19. Stewart BJ, McCarter LL. Lateral flagellar gene system of *Vibrio parahaemolyticus*. *J Bacteriol*. 2003;185:4508-4518.
20. Aagesen AM, Phuvasate S, Su YC, Hase CC. Persistence of *Vibrio parahaemolyticus* in the Pacific oyster, *Crassostrea gigas*, is a multifactorial process involving pili and flagella but not type III secretion systems or phase variation. *Appl Environ Microbiol*. 2013;79:3303-3305.
21. Yanagihara I, Nakahira K, Yamane T, et al. Structure and functional characterization of *Vibrio parahaemolyticus* thermostable direct hemolysin. *J Biol Chem*. 2010;285:16267-16274.
22. Yu Y, Fang L, Zhang Y, Sheng H, Fang W. VgrG2 of type VI secretion system 2 of *Vibrio parahaemolyticus* induces autophagy in macrophages. *Front Microbiol*. 2015;6:168.
23. Zheng J, Tung SL, Leung KY. Regulation of a type III and a putative secretion system in *Edwardsiella tarda* by EsrC is under the control of a two-component system, EsrA-EsrB. *Infect Immun*. 2005;73:4127-4137.
24. Philippe N, Alcaraz JP, Coursange E, Geiselmann J, Schneider D. Improvement of pCVD442, a suicide plasmid for gene allele exchange in bacteria. *Plasmid*. 2004;51:246-255.
25. Tissenbaum HA. Genetics, life span, health span, and the aging process in *Caenorhabditis elegans*. *J Gerontol A Biol Sci Med Sci*. 2012;67:503-510.
26. Peleg AY, Tampakakis E, Fuchs BB, Eliopoulos GM, Moellering RC Jr, Mylonakis E. Prokaryote-eukaryote interactions identified by using *Caenorhabditis elegans*. *Proc Natl Acad Sci U S A*. 2008;105:14585-14590.
27. Moy TI, Ball AR, Anklesaria Z, Casadei G, Lewis K, Ausubel FM. Identification of novel antimicrobials using a live-animal infection model. *Proc Natl Acad Sci U S A*. 2006;103:10414-10419.
28. Aballay A, Yorgey P, Ausubel FM. *Salmonella typhimurium* proliferates and establishes a persistent infection in the intestine of *Caenorhabditis elegans*. *Curr Biol*. 2000;10:1539-1542.
29. Sawabe T, Fukui Y, Stabb EV. Simple conjugation and outgrowth procedures for tagging vibrios with GFP, and factors affecting the stable expression of the gfp tag. *Lett Appl Microbiol*. 2006;43:514-522.
30. Zhang Y, Faucher F, Zhang W, et al. Structure-guided disruption of the pseudopilus tip complex inhibits the type II secretion in *Pseudomonas aeruginosa*. *PLoS Pathog*. 2018;14:e1007343.
31. Wingett SW, Andrews S. FastQ screen: a tool for multi-genome mapping and quality control. *F1000Res*. 2018;7:1338.
32. Kim D, Pertea G, Trapnell C, Pimentel H, Kelley R, Salzberg SL. TopHat2: accurate alignment of transcriptomes in the presence of insertions, deletions and gene fusions. *Genome Biol*. 2013;14:R36.
33. Love MI, Huber W, Anders S. Moderated estimation of fold change and dispersion for RNA-seq data with DESeq2. *Genome Biol*. 2014;15:550.
34. Zhang L, Krachler AM, Broberg CA, et al. Type III effector VopC mediates invasion for Vibrio species. *Cell Rep*. 2012;1:453-460.
35. Jaskolska M, Stutzmann S, Stoudmann C, Blokesch M. QstR-dependent regulation of natural competence and type VI secretion in *Vibrio cholerae*. *Nucleic Acids Res*. 2018;46:10619-10634.
36. Fan X, Lamarre-Vincent N, Wang Q, Struhl K. Extensive chromatin fragmentation improves enrichment of protein binding sites in chromatin immunoprecipitation experiments. *Nucleic Acids Res*. 2008;36:e125.
37. Salomon D, Gonzalez H, Updegraff BL, Orth K. *Vibrio parahaemolyticus* type VI secretion system 1 is activated in marine conditions to target bacteria, and is differentially regulated from system 2. *PLoS ONE*. 2013;8:e61086.
38. Zhang Q, Dong X, Chen B, Zhang Y, Zu Y, Li W. Zebrafish as a useful model for zoonotic *Vibrio parahaemolyticus* pathogenicity in fish and human. *Dev Comp Immunol*. 2016;55:159-168.
39. Durai S, Karutha Pandian S, Balamurugan K. Changes in *Caenorhabditis elegans* exposed to *Vibrio parahaemolyticus*. *J Microbiol Biotechnol*. 2011;21:1026-1035.
40. Babitzke P, Romeo T. CsrB sRNA family: sequestration of RNA-binding regulatory proteins. *Curr Opin Microbiol*. 2007;10:156-163.
41. Dorman MJ, Dorman CJ. Regulatory hierarchies controlling virulence gene expression in *Shigella flexneri* and *Vibrio cholerae*. *Front Microbiol*. 2018;9:2686.
42. Feng L, Rutherford ST, Papenfort K, et al. A Qrr noncoding RNA deploys four different regulatory mechanisms to optimize quorum-sensing dynamics. *Cell*. 2015;160:228-240.
43. Huang L, Hu J, Su Y, et al. Genome-wide detection of predicted non-coding RNAs related to the adhesion process in *Vibrio alginolyticus* using high-throughput sequencing. *Front Microbiol*. 2016;7:619.
44. Kuehn MJ, Kesty NC. Bacterial outer membrane vesicles and the host-pathogen interaction. *Genes Dev*. 2005;19:2645-2655.
45. Song T, Mika F, Lindmark B, et al. A new *Vibrio cholerae* sRNA modulates colonization and affects release of outer membrane vesicles. *Mol Microbiol*. 2008;70:100-111.
46. Heeb S, Haas D. Regulatory roles of the GacS/GacA two-component system in plant-associated and other gram-negative bacteria. *Mol Plant Microbe Interact*. 2001;14:1351-1363.
47. Alteri CJ, Himpsl SD, Engstrom MD, Mobley HL. Anaerobic respiration using a complete oxidative TCA cycle drives multicellular swarming in *Proteus mirabilis*. *mBio*. 2012;3:00365.
48. Hensel M, Hinsley AP, Nikolaus T, Sawers G, Berks BC. The genetic basis of tetrathionate respiration in *Salmonella typhimurium*. *Mol Microbiol*. 1999;32:275-287.
49. Winter SE, Thiennimitr P, Winter MG, et al. Gut inflammation provides a respiratory electron acceptor for *Salmonella*. *Nature*. 2010;467:426-429.
50. Pan X, Dong Y, Fan Z, et al. In vivo host environment alters *Pseudomonas aeruginosa* susceptibility to aminoglycoside antibiotics. *Front Cell Infect Microbiol*. 2017;7:83.
51. Cambi A, Figdor C. Necrosis: C-type lectins sense cell death. *Curr Biol*. 2009;19:R375-R378.
52. Bai C, Sen P, Hofmann K, et al. SKP1 connects cell cycle regulators to the ubiquitin proteolysis machinery through a novel motif, the F-box. *Cell*. 1996;86:263-274.
53. Zhang R, Wu L, Eckert T, et al. Lysozyme's lectin-like characteristics facilitates its immune defense function. *Q Rev Biophys*. 2017;50:e9.
54. Surana P, Gowda CM, Tripathi V, Broday L, Das R. Structural and functional analysis of SMO-1, the SUMO homolog in *Caenorhabditis elegans*. *PLoS ONE*. 2017;12:e0186622.
55. Flotho A, Melchior F. Sumoylation: a regulatory protein modification in health and disease. *Annu Rev Biochem*. 2013;82:357-385.

56. Tabara H, Hill RJ, Mello CC, Priess JR, Kohara Y. pos-1 encodes a cytoplasmic zinc-finger protein essential for germline specification in *C. elegans*. *Development*. 1999;126:1-11.
57. Sonnichsen B, Koski LB, Walsh A, et al. Full-genome RNAi profiling of early embryogenesis in *Caenorhabditis elegans*. *Nature*. 2005;434:462-469.
58. Lublin AL, Evans TC. The RNA-binding proteins PUF-5, PUF-6, and PUF-7 reveal multiple systems for maternal mRNA regulation during *C. elegans* oogenesis. *Dev Biol*. 2007;303:635-649.
59. Ermolaeva MA, Schumacher B. Insights from the worm: the C. elegans model for innate immunity. *Semin Immunol*. 2014;26:303-309.
60. Alper S, McBride SJ, Lackford B, Freedman JH, Schwartz DA. Specificity and complexity of the *Caenorhabditis elegans* innate immune response. *Mol Cell Biol*. 2007;27:5544-5553.
61. Ermolaeva M, Schumacher B. The innate immune system as mediator of systemic DNA damage responses. *Commun Integr Biol*. 2013;6:e26926.
62. Kim DH, Feinbaum R, Alloing G, et al. A conserved p38 MAP kinase pathway in *Caenorhabditis elegans* innate immunity. *Science*. 2002;297:623-626.
63. Liberati NT, Fitzgerald KA, Kim DH, Feinbaum R, Golenbock DT, Ausubel FM. Requirement for a conserved Toll/interleukin-1 resistance domain protein in the *Caenorhabditis elegans* immune response. *Proc Natl Acad Sci U S A*. 2004;101:6593-6598.
64. Evans EA, Kawli T, Tan MW. *Pseudomonas aeruginosa* suppresses host immunity by activating the DAF-2 insulin-like signaling pathway in *Caenorhabditis elegans*. *PLoS Pathog*. 2008;4:e1000175.
65. Alegado RA, Tan MW. Resistance to antimicrobial peptides contributes to persistence of *Salmonella typhimurium* in the C. elegans intestine. *Cell Microbiol*. 2008;10:1259-1273.
66. O'Rourke D, Baban D, Demidova M, Mott R, Hodgkin J. Genomic clusters, putative pathogen recognition molecules, and antimicrobial genes are induced by infection of *C. elegans* with *M. nematophilum*. *Genome Res*. 2006;16:1005-1016.
67. Urano F, Calfon M, Yoneda T, et al. A survival pathway for *Caenorhabditis elegans* with a blocked unfolded protein response. *J Cell Biol*. 2002;158:639-646.
68. Matlawska-Wasowska K, Finn R, Mustel A, et al. The *Vibrio parahaemolyticus* type III secretion systems manipulate host cell MAPK for critical steps in pathogenesis. *BMC Microbiol*. 2010;10:329.
69. Finn R, Ahmad T, Coffey ET, Brayden DJ, Baird AW, Boyd A. Translocation of *Vibrio parahaemolyticus* across an in vitro M cell model. *FEMS Microbiol Lett*. 2014;350:65-71.
70. Cheesman HK, Feinbaum RL, Thekkiniath J, Dowen RH, Conery AL, Pukkila-Worley R. Aberrant activation of p38 MAP kinase-dependent innate immune responses is toxic to *Caenorhabditis elegans*. *G3 (Bethesda)*. 2016;6:541-549.
71. Fletcher M, Tillman EJ, Butty VL, Levine SS, Kim DH. Global transcriptional regulation of innate immunity by ATF-7 in C. elegans. *PLoS Genet*. 2019;15:e1007830.
72. Zhou X, Gewurz BE, Ritchie JM, et al. A *Vibrio parahaemolyticus* T3SS effector mediates pathogenesis by independently enabling intestinal colonization and inhibiting TAK1 activation. *Cell Rep*. 2013;3:1690-1702.
73. Trosky JE, Mukherjee S, Burdette DL, et al. Inhibition of MAPK signaling pathways by VopA from *Vibrio parahaemolyticus*. *J Biol Chem*. 2004;279:51953-51957.
74. Burdette DL, Yarbrough ML, Orvedahl A, Gilpin CJ, Orth K. *Vibrio parahaemolyticus* orchestrates a multifaceted host cell infection by induction of autophagy, cell rounding, and then cell lysis. *Proc Natl Acad Sci U S A*. 2008;105:12497-12502.
75. Ho BT, Dong TG, Mekalanos JJ. A view to a kill: the bacterial type VI secretion system. *Cell Host Microbe*. 2014;15:9-21.
76. Romeo T, Vakulskas CA, Babitzke P. Post-transcriptional regulation on a global scale: form and function of Csr/Rsm systems. *Environ Microbiol*. 2013;15:313-324.
77. Mey AR, Butz HA, Payne SM. *Vibrio cholerae* CsrA regulates ToxR levels in response to amino acids and is essential for virulence. *mBio*. 2015;6:e01064.
78. Papenfort K, Vogel J. Small RNA functions in carbon metabolism and virulence of enteric pathogens. *Front Cell Infect Microbiol*. 2014;4:91.
79. Kulkarni PR, Cui X, Williams JW, Stevens AM, Kulkarni RV. Prediction of CsrA-regulating small RNAs in bacteria and their experimental verification in *Vibrio fischeri*. *Nucleic Acids Res*. 2006;34:3361-3369.
80. Gooderham WJ, Hancock RE. Regulation of virulence and antibiotic resistance by two-component regulatory systems in *Pseudomonas aeruginosa*. *FEMS Microbiol Rev*. 2009;33:279-294.

SUPPORTING INFORMATION

Additional Supporting Information may be found online in the Supporting Information section.

How to cite this article: Zhang W, Xie R, Zhang XD, et al. Organism dual RNA-seq reveals the importance of BarA/UvrY in *Vibrio parahaemolyticus* virulence. *The FASEB Journal*. 2020;34:7561–7577. https://doi.org/10.1096/fj.201902630R